3D PRINTING AND STRUCTURAL TESTING OF QUICK CONNECTIONS

Kee Young Jung, B.S.
Civil Engineering Honors

CE 679HB
Engineering Honors Program
The University of Texas at Austin

May 6th, 2018

_____

Prof. Patricia Clayton, Ph.D.
Cockrell School of Engineering
Supervising Professor

_____

Prof. Raissa Ferron, Ph.D., P.E.
Cockrell School of Engineering
Second Reader

3D PRINTING AND STRUCTURAL TESTING OF QUICK CONNECTIONS

Table of Contents

1. INTRODUCTION

3D printing technology allows three-dimensional solid objects to be created from a digital file. It is an additive manufacturing process that creates objects by laying down successive layers of material in one continuous process. The use of 3D printing has been explored in many different industries due to its potential to revolutionize the manufacturing process. The construction industry is not an exception to this trend as it is going through a major change associated with the automation of the construction process. 3D printing offers the construction industry a possibility of creating construction elements of unique, complex geometry that can be custom-made and mass-produced.

This study aims to utilize the benefits of the 3D printer by printing connection members of complex geometry inspired from Japanese woodworking and the modern proprietary connection from the ConXTech. The connection models will be tested for its strength and serviceability and their performance will be analyzed to assess the connection's potential for structural and non-structural application. By combining the "fastener-free" and the "quick and easy to connect" abilities of the wooden joineries and the ConXTech connections with the benefit of the 3D printing technology, the study will explore the process of innovation that can result from interdisciplinary research.

2. BACKGROUND

Ever since people started creating objects, they explored different ways to connect pieces of materials to create a bigger form. From spears to chairs to houses, most manmade objects contain at least one connecting part. This section will introduce wood and steel as two main materials used as structural connection elements. The characteristics of each type of joinery and how they inspired the connections developed in this study will be explained.

2.1. Wood-to-wood joinery

Historically, wood has been used for variety of applications such as building frames, flooring, furniture, hand tools, and toys due to its widespread availability. Wood joinery is necessary to connect multiple pieces of wood in these applications. There are several types of joints, such as a splice joint, which connects the two ends of wooden pieces together to form a longer piece, or a butt joint, which connects two pieces at a 90-degree angle, as shown in Figure 1. These joints can be held in place using various types of glue or fasteners such as nails, screws, staples, or bolts, or it can be "fastener-free" if it does not have any fasteners. Commonly, the fastener-free joints have basic components of a mortise (i.e., a hole) hole for the tenon (protruded part) to be inserted (see Figure 2).
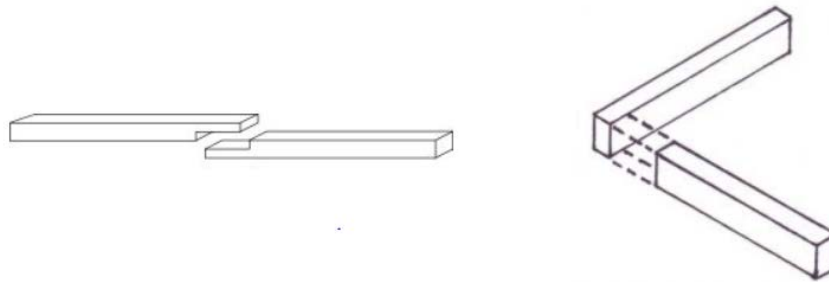

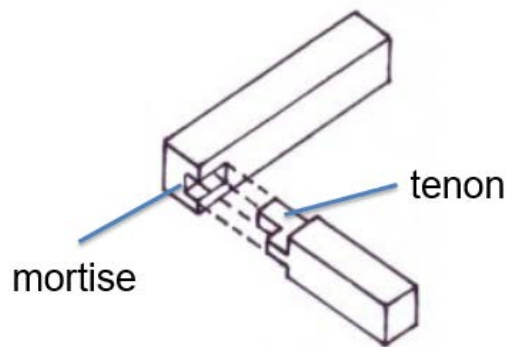*Figure 1: Splice joint (left) and butt joint (right)[1]*

Figure 2: Mortise and Tenon [2]

There are several construction benefits to using fastener-free wood joints. First, it reduces the assembly time as parts are joined simply by being slid into one another. Additionally, it is relatively easy to replace damaged parts. The problem of corrosion is avoided as metal fasteners are not used in the structure [3]. The use of chemical preservatives is also avoided because no epoxy or other polymer

adhesives are needed to fill holes when adhering the fastener or as the fastener itself. Overall, it can enhance the aesthetics of the structure by exposing the full side of the wood.

Fastener-free connections are not a modern invention. The Japanese have long been perfecting their traditional wood joints of complex geometry through their complicated manufacturing processes. Elaborate wooden craftsmanship became popular in Japan in the 6th century with the introduction of Buddhism. Beginning with Prince Shotoku, Japanese rulers commissioned the construction of large temples and pagodas such as the Horyuji Temple (Figure 3) to promote the teachings of Buddhism. Scarcity of good timber forced architects to splice short timbers for truss construction for these large structures and they came up with various ways to splice timber.
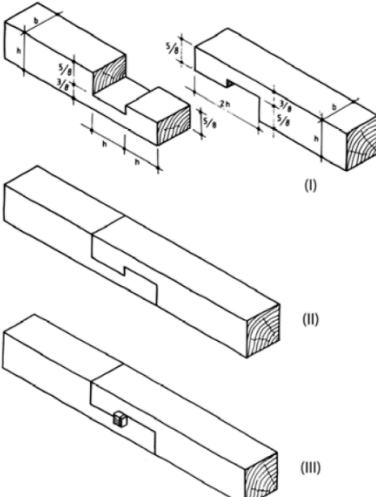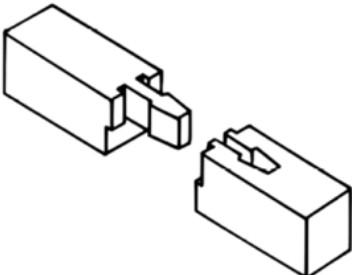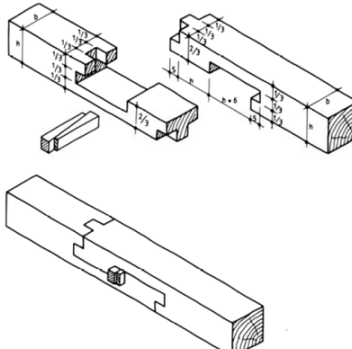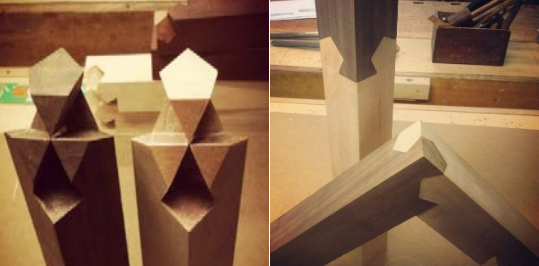

Figure 3: Horyuji Temple in Nara, Japan [4]

Many joineries that were independently developed in different regions of the world have similar configurations. For example, a shiguchi is a Japanese joint that joins two elements at a right angle and is equivalent to the European cross lap joint. A tsugite is a Japanese splice joint that join end to end and is similar to the European half lap joint. Table 1 lists the specific splice joints that inspired the work in this thesis.

Table 1: Types of splice joints and their characteristics [5]

Name and Origin	Characteristic	Figure
• Shippasami-tsugi (Japan)	Has 1 or 2 tooth as a mortise, designed to resist force from all direction	

• Kanawa-tsugi (Japan) • Hakenblatt (Germany)	A cogged lap joint with straight shoulders	
• Kama-tsugi (Japan) • Gooseneck or Forked tenon joint (France) • Pfostenzange/ Ständerzange (Germany)	First appeared in Heian period (794-1185), geometrically optimized during the Edo period (1603-1868) due to the improvement in tool quality	
• Shiribasami-tsugi (Japan) • Lock joint (France) • Französisches Schloß (Germany)	Has 1 tooth on the surface of the joint	
• Kawaii-tsugite (Japan)	Modern wood joint created by a Professor at Tokyo University and later recreated by a woodworking student Shinobu Kobayashi. This form of joinery has a complex geometry and can be rearranged in 3 different ways; either a straight joint or 2 corner joints [6]	

2.2. Steel-to-steel connections

Steel members are typically connected via bolts and/or welds onsite. Welding requires a skilled laborer to use an electric arc to generate heat to melt the filler material to attach to each face of a metal.

Figure 4: Bolted column splice (left)[7] and welding of steel connection (right)[8]

The ConXtech connection is a proprietary connection that facilitates the easy fit-up of connections. While they are not "fastener-free" like the wood joinery previously discussed, they do reduce the number of required bolts and rely on connection geometry to help transfer the loads through the connection like the fastener-free wood joinery. ConXtech connections were developed by ConXtech Inc., which is a privately-held construction technology company in Pleasanton, CA. It is a prefabricated steel connection that is simply lowered and locked into place and then fixed by installing collar bolts, as shown in Figure 5. These connections are moment resisting and are approved for use in seismic applications by the American Institute of Steel Construction (AISC).
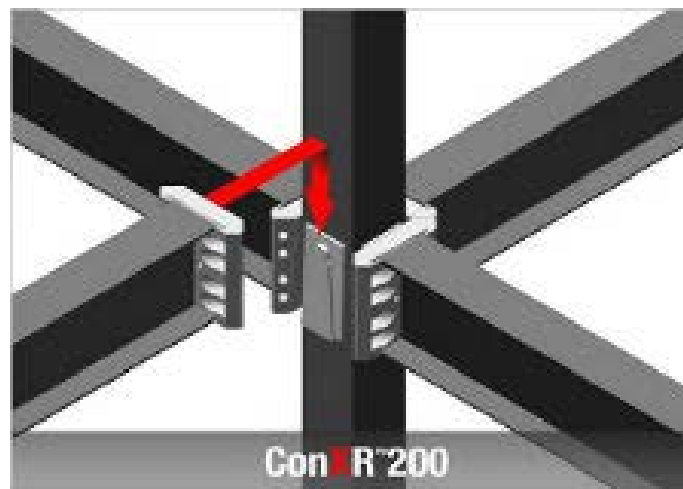

Figure 5: ConXR Connection [9]

This study will test three models inspired from the wood joineries and the steel connection. Two of the models are named after the traditional Shippasami-tsugi and the modern Kawaii-tsugite wood joint. These joints will be 3D printed in plastic. Yet 3D printed objects have similar properties to the anisotropic behavior of the wood. As wood exhibits a high tensile and compressive strength to weight ratio in the direction of the wood grain, with a low tensile capacity perpendicular to the grain [10], the 3D printed objects are strong in the direction of the printed layer and having low tensile capacity perpendicular to the layer. The third model is named after the ConXR Connection, with a slight modification to its mortise and

tenon geometry. All three models are labeled as a "quick" connection due to their ability to connect easily by hand.

3. Modelling and Printing of Test Models in 3D

Three "quick" connections inspired by the connections discussed in the background section (Chapter 2), were designed and manufactured to be tested for flexure. These modified versions of the Kawaii tsugite, Shippasami-tsugi, and the ConXR connections were designed to form a 1.5in x 1.5in x 10in beam when two pieces are assembled. Three specimens of each of the three connection types were printed and tested. In this study, CraftBotXL printers at the Longhorn MakerStudio were used with the CraftWare slicer software to generate suitable models for 3D printing. A detailed description of the process of generating 3D models suitable for printing is given in Appendix A.

3.1. Specimen Preparation

The specimens were printed with a standard layer thickness of 0.008 inches [0.2 mm] and an infill density of 70 percent instead of a 100 percent solid infill to reduce printing time while maintaining a high density for strength testing. Infill density is defined by the percentage of the volume of the printed object that is solid and not void. All our models had a gap of 0.005 inches between parts in the connections to provide tolerances for easy fit-up. Average printing time was around 21 hours for each specimen. A total of 12 specimens - three specimens for each three final connection models and three regular 70% infill solid beams for comparison - were printed for this test. Through rapid prototyping, tolerances and the final geometry of the models were perfected, as shown in Figure 6. All the specimens were printed with PLA filament.
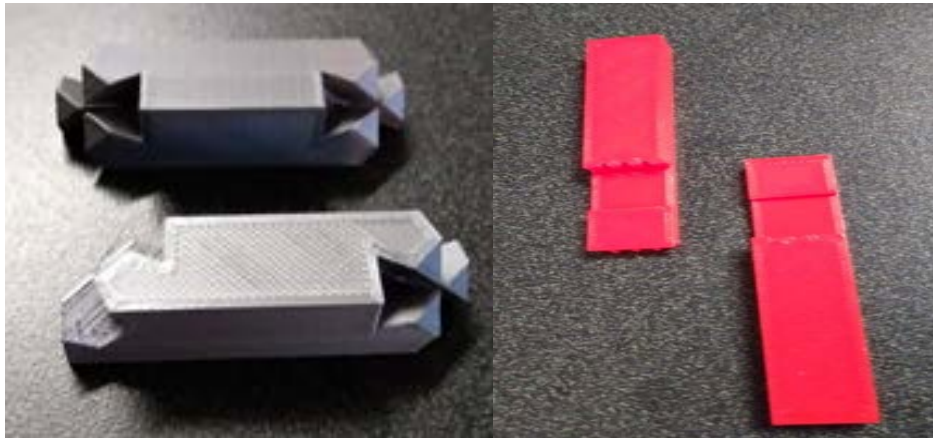

Figure 6: Prototype of Kawaii (left) and Shippasami (right)

3.1.1. Kawaii Model

The Kawaii model had an estimated printing time of 21 hours and a connection length of 1.5 inches.
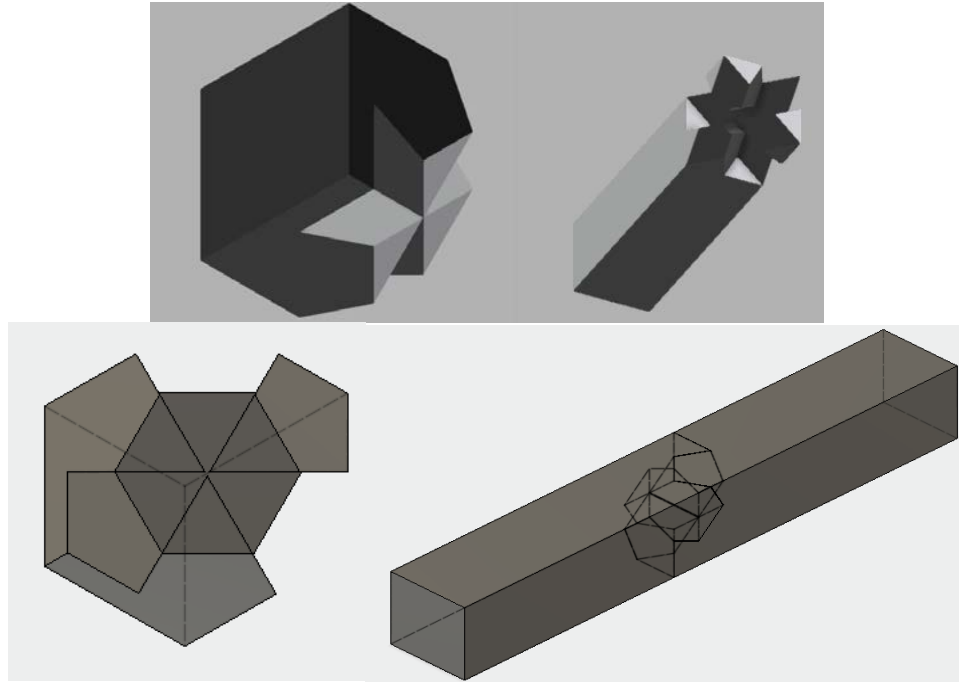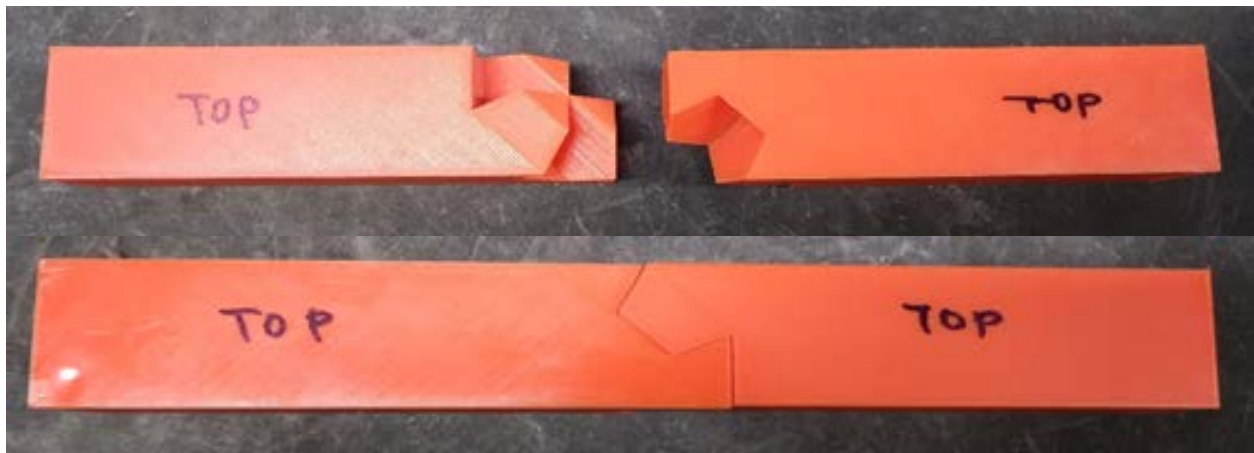
Figure 7: 3D Modelling of Kawaii connection

Figure 8: Final print of Kawaii model before (top) and after (bottom) connecting

3.1.2. Shippasami Model

The Shippasami model had an estimated printing time of 22 hours and a connection length of 3 inches. The 3D models of the connection are shown in Figure 9. A raft was added to the bottom to prevent warping of the specimen during printing and a support was auto-generated from Craftware in places where the connection parts are hanging off the main body, as shown in Figure 10. After the specimen was printed, the supports were removed using a pinch off tool and the rugged parts were smoothened using hand tools, as shown in Figure 11. Then the two parts were joined and the pin was inserted in the hole to complete the assembly, as shown in Figure 12.

Figure 9: 3D Modelling of Shippasami model
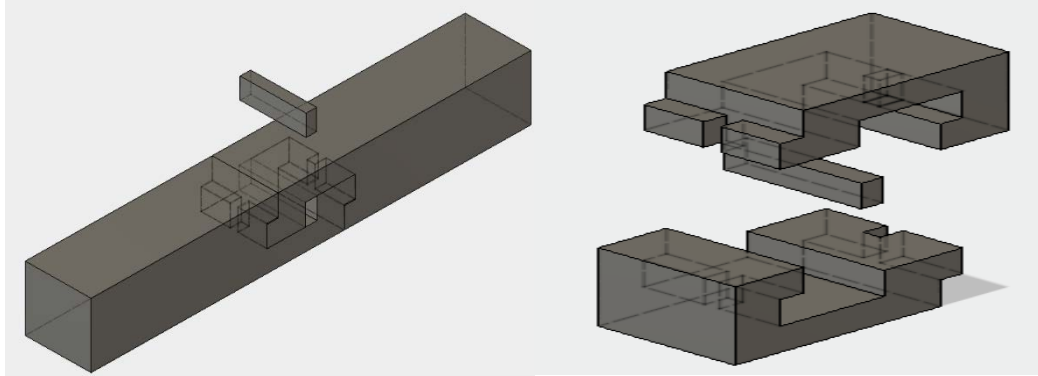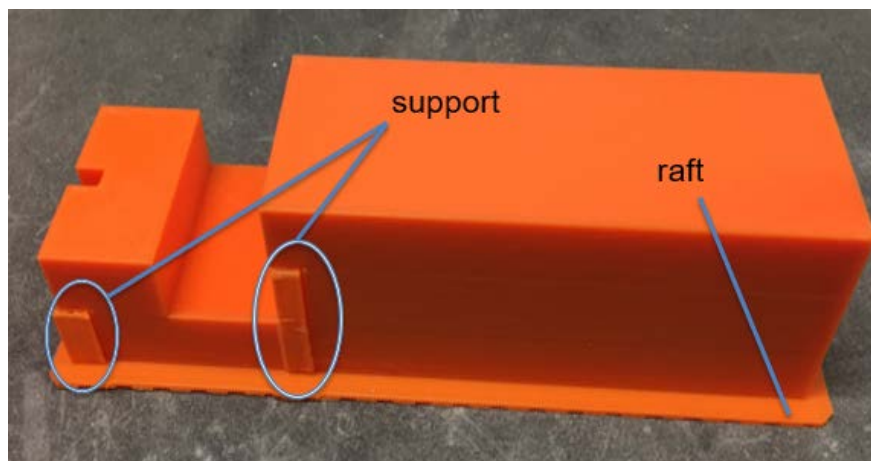

Figure 10: A raft was added to the bottom to prevent warping of the specimen during printing and a support was auto-generated from CraftWare in places where the connection parts are hanging off the main body.
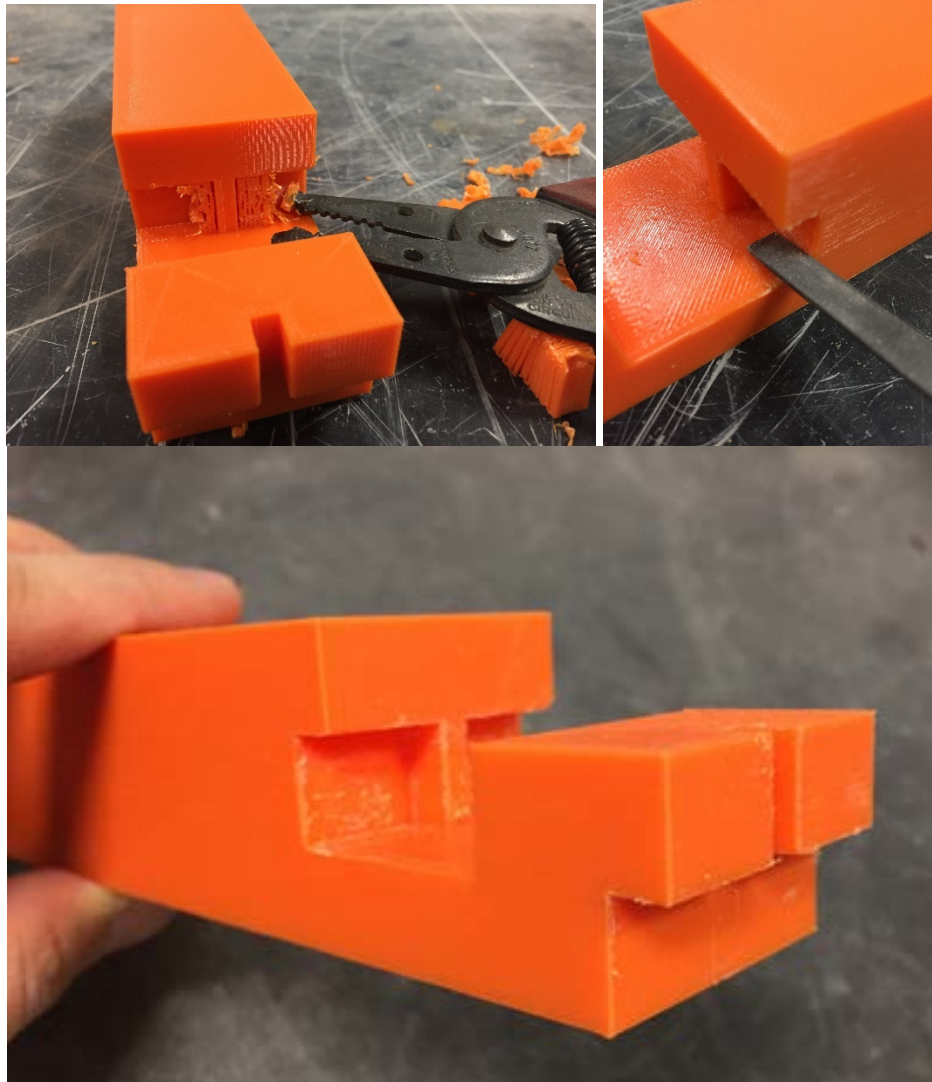
Figure 11: After the specimen was printed, the supports were removed using a pinch off tool (top left) and the rugged parts were smoothened using hand tools (top right).

a)

b)

c)

d)
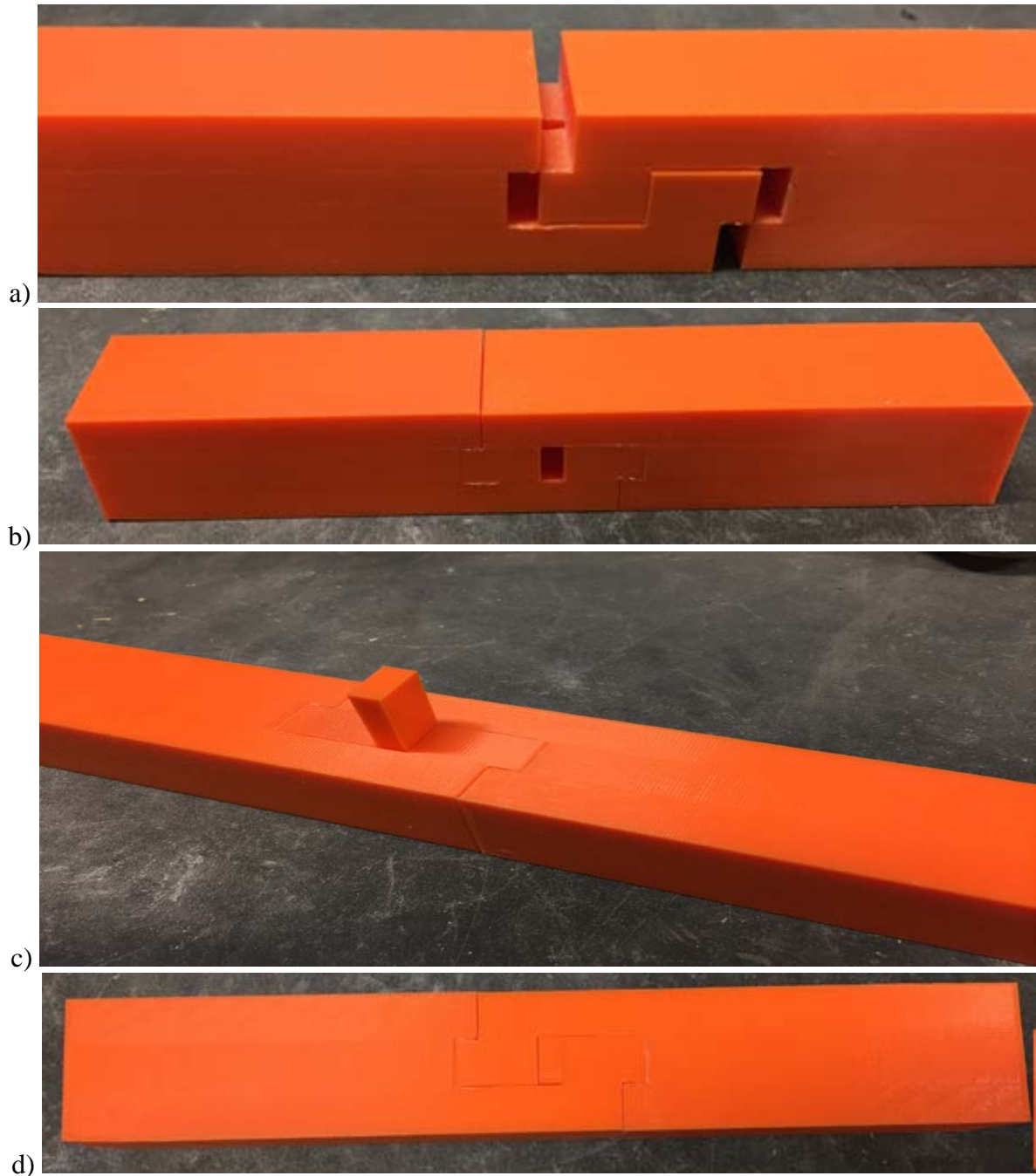
Figure 12: Two connections were joined (a,b) and the pin was inserted in the hole (c) to complete the assembly (d).

3.1.3. ConXTech Model

The ConXTech model had an estimated printing time of 21.5 hours and a connection length of 0.55 inches. The 3d models are shown in Figure 13. The model also had supports auto generated from CraftWare that were removed by hand tools. The connection with the rounded part was inserted into the connection with the socket looking end, as shown in Figure 15.

Figure 13: 3D Modelling of ConXTech model

Figure 14: Printing of ConXTech model

Figure 15: Final print of ConXTech model before (top) and after (bottom) connecting

3.2 Printing Failures

As expected from an emerging technology such as 3D printing, failures can, and did, occur during the printing process. We experienced issues mainly with layer shift, warping, and smudging of the specimen due to many reasons. Further information about these various types of failures and methods to mitigate them are discussed below.
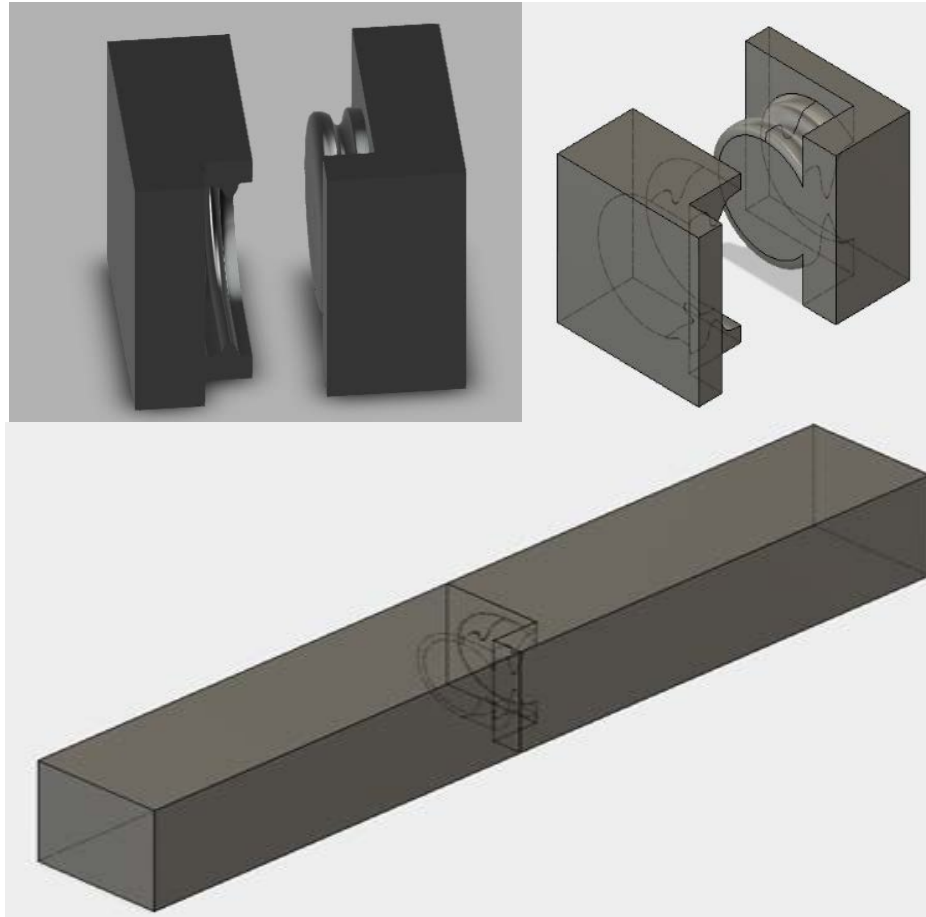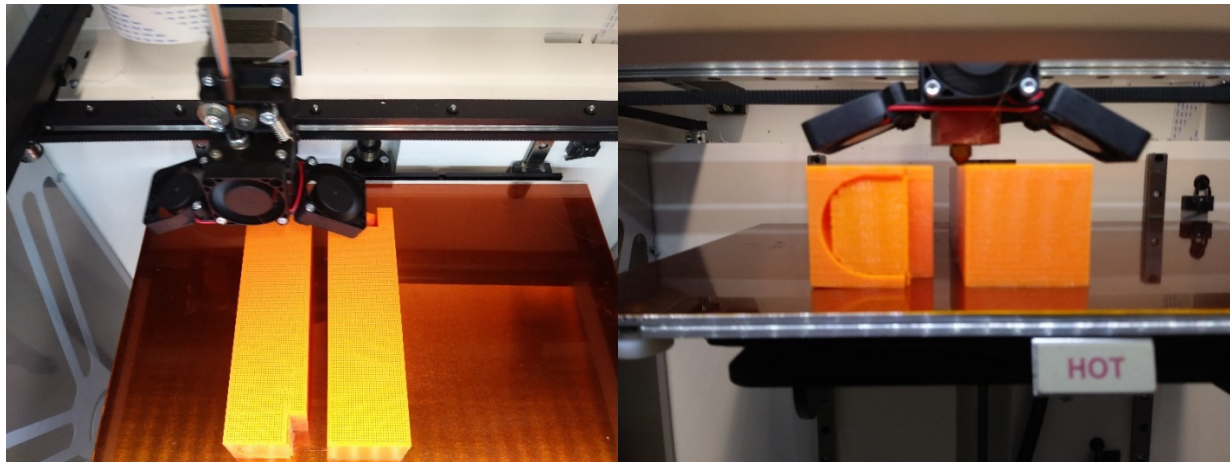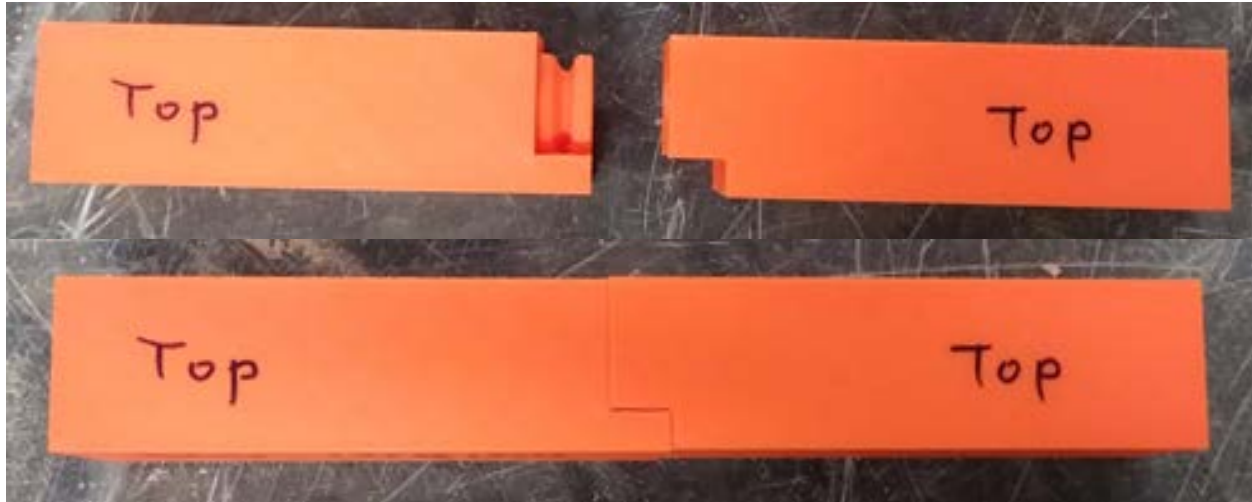
Layer shift failure occurred because the printer head was moving too fast that it did not allow the nozzle to extrude the polymer at the exact location. When the printer head skipped a layer without extruding the material, it created a layer shift and moved the future layers horizontally offset to where they were supposed to be placed. This often caused the specimen to collapse when the layer shift added too much weight and unsupported overhangs to one side of the specimen. This issue was solved by adjusting the printing speed within the CraftWare software.

Figure 16: Failure by layer shift, notice the gap between the two protruding lines at the edge

One of the main reason for the warping failure is that the first layer of the specimen is not fully and uniformly attached to the bed platform. When any part of the bottom of the specimen is detached from the bed, it prevents the next layers from being printed on a level plane, which created unwanted

stresses on certain parts of the specimen. Also, when there is a gap between the first layer and the bed platform, hot air will enter the space and expand under the specimen and exacerbate the warping issue. This issue of warping was easily prevented by allowing the bed platform to be covered fully with a thick layer of hair spray before the print started. It does not seem to matter whether the hair spray is applied before or after the bed platform is heated.

Another cause of warping was observed during the winter season due to the cold ambient temperature around the printer. As soon as the polymer was extruded from the nozzle, it cooled at such a rapid rate that it caused the polymer to solidify and shrink before it was properly attached to the layer below and next to it. This issue was solved by adjusting the room temperature of work space and placing the printer far away from any possible inlet of cold air such as a door, window, or air conditioning vent.

Figure 17: Failures by warping

A specimen experienced collapse when the support was not strong enough to hold up the hanging parts during the printing. Since all specimens had to be printed in one layer orientation for testing, some parts of the specimens were to be printed as hanging parts. This issue was solved by increasing the support infill in the CraftWare before printing.
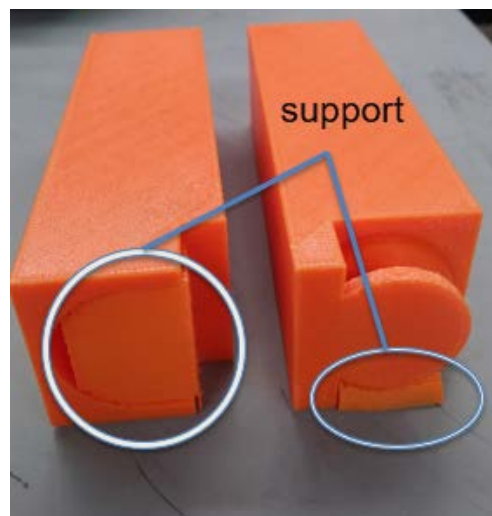

Figure 18: Auto-generated supports for the ConXTech model

Smudging happened when the printer head too close to the bed platform during printing and prevented the layers from extruding properly. This issue was observed mainly at the beginning of printing

when the first layer was not visible because it was smudged to the bed and spread out thinly to the sides, as shown in Figure 19. This issue was solved by leveling the bed before the printing, which was done by personnel at the Maker Studio.
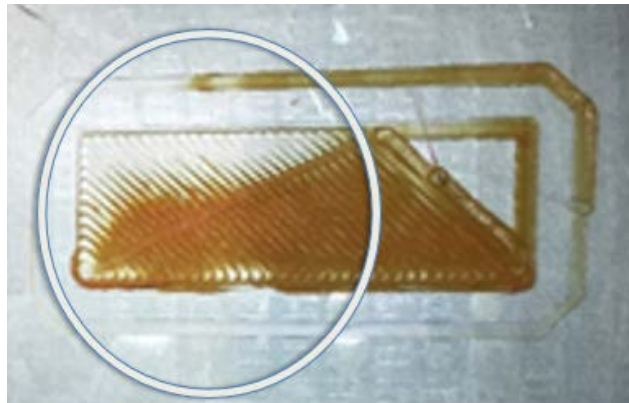
Figure 19: Failure to print a pin for the Shippasami model due to smudging

Stringing occurred when the printer head was moving too fast that it did not allow the layers to cool and stay in place. It was a minor problem since the strings were easily removed from the specimen using a hand tool.
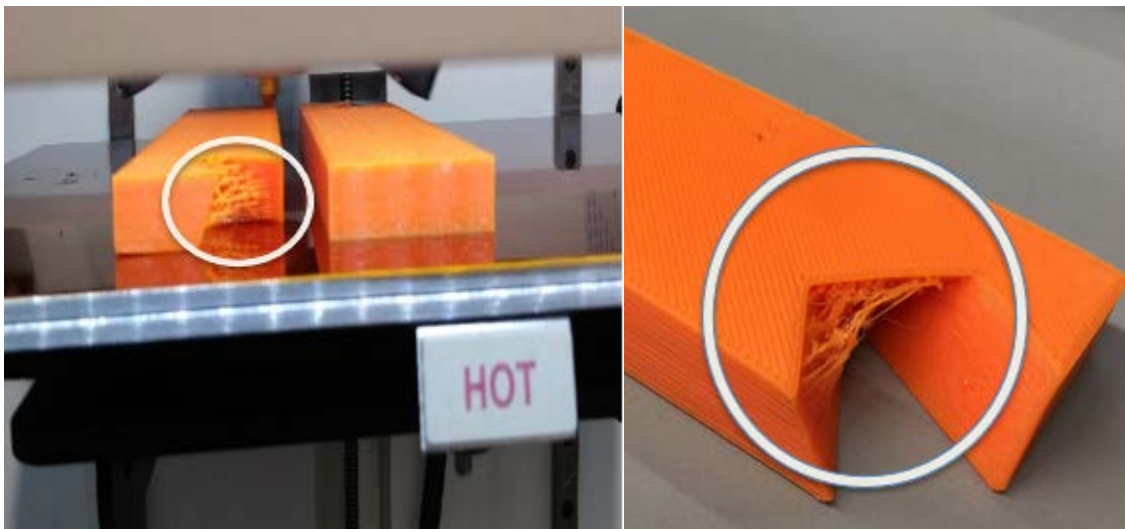
Figure 20: Stringing of the Kawaii model

Tolerance failure is when the connecting parts did not fit perfectly. As shown in Figure 21, the connecting surface is not smooth but instead has one part protruding outwards. This issue was created when the two joints were printed one at a time or were printed at the same time but cooled at a different rate. Tolerance failure is a difficult issue because if the tolerance is increased even a small amount to account for these failures, the printed joints will be too loose and not stay in place once they were connected. Therefore, when the tolerance became an issue, the connections were simply reprinted.

Figure 21: Tolerance issue of the printed Kawaii model

3.3 Selecting a Print Material
      While there are different types of desktop printers and print materials available for the public, the specimens were printed in PLA(Polylactic Acid) for this test as it was the most common material used for desktop printing.

4. Test Set-Up

Four-point bending tests were conducted to determine the flexural strength of three, deflection, and failure mode of the 3D printed connections.

4.1. Four Point Bending Test

To test the flexural strength of each connection, a four-point bending test was used, where the connection of interest was located at the middle of the beam in the region of maximum flexural demand as shown in Figure 22 c. As shown in Figure 22 a, four-point bending test consist of placing a beam with a bottom span length of L and a top span length of L/2. Constant loading rate is applied to the specimen until it fails. A valid test is one in which the specimen cracks within the bottom of the beam within the inner span range (shown the region denoted as L/2 in Figure 22a) since this is where the maximum moment occurs.
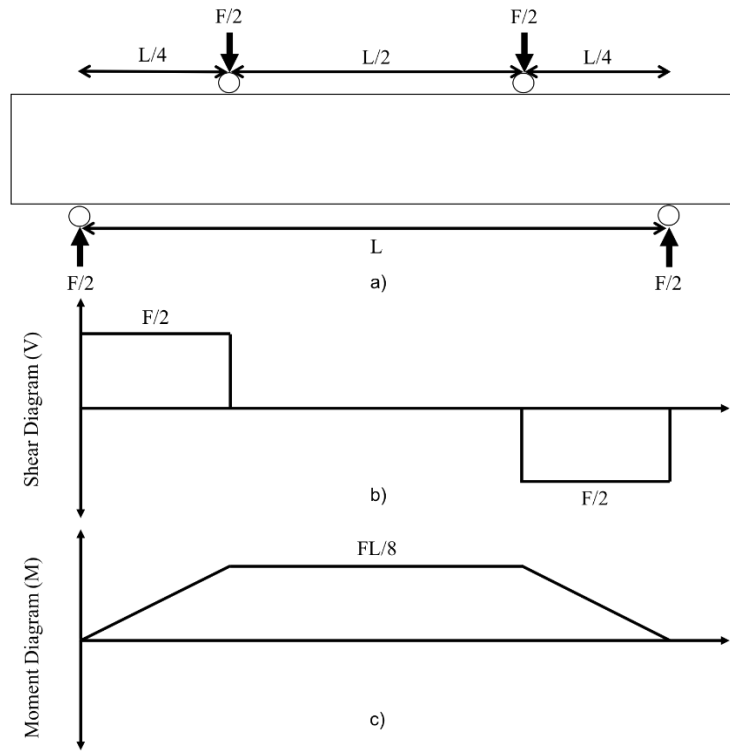
Figure 22: Shear and moment diagram for a four-point bending test
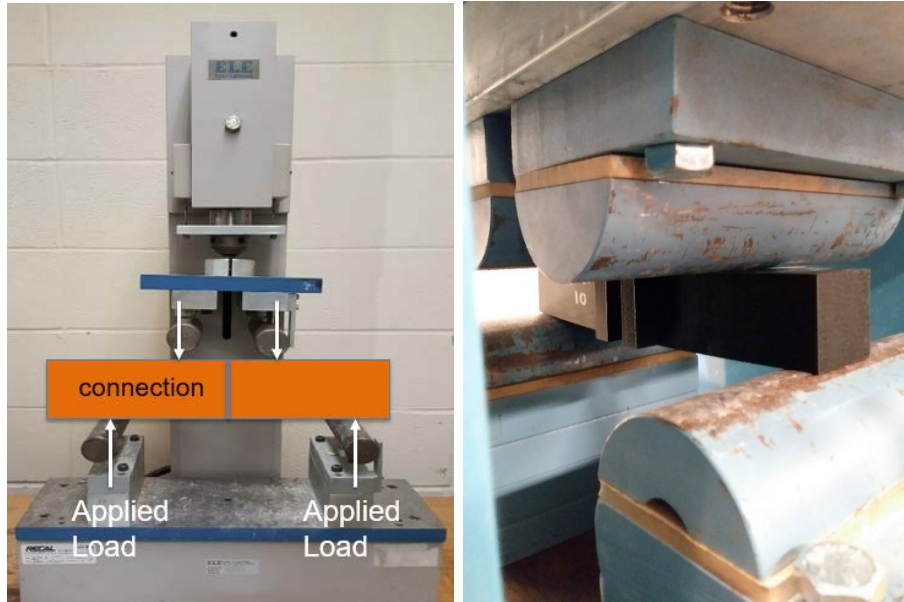
Figure 23: Free-body diagram of the four-point bending test (left) and the loading of the specimen using the Forney compression machine (right)

Instead of the standard compression test set-up, the loading platform was replaced with a custom made flexural test assembly. The test set-up consists of top plate that has two points of contacts that are 4 inches (101.6 mm) apart and a bottom plate with two raised contact points that are 8 inches (203.2 mm) apart from the centerline of each cylinder. The bottom plate is on top of a steel channel for an additional height.

101.6mm

Four-point bending set-up

GoPro Camera

Linear Potentiometer

Specimen

203.2mm
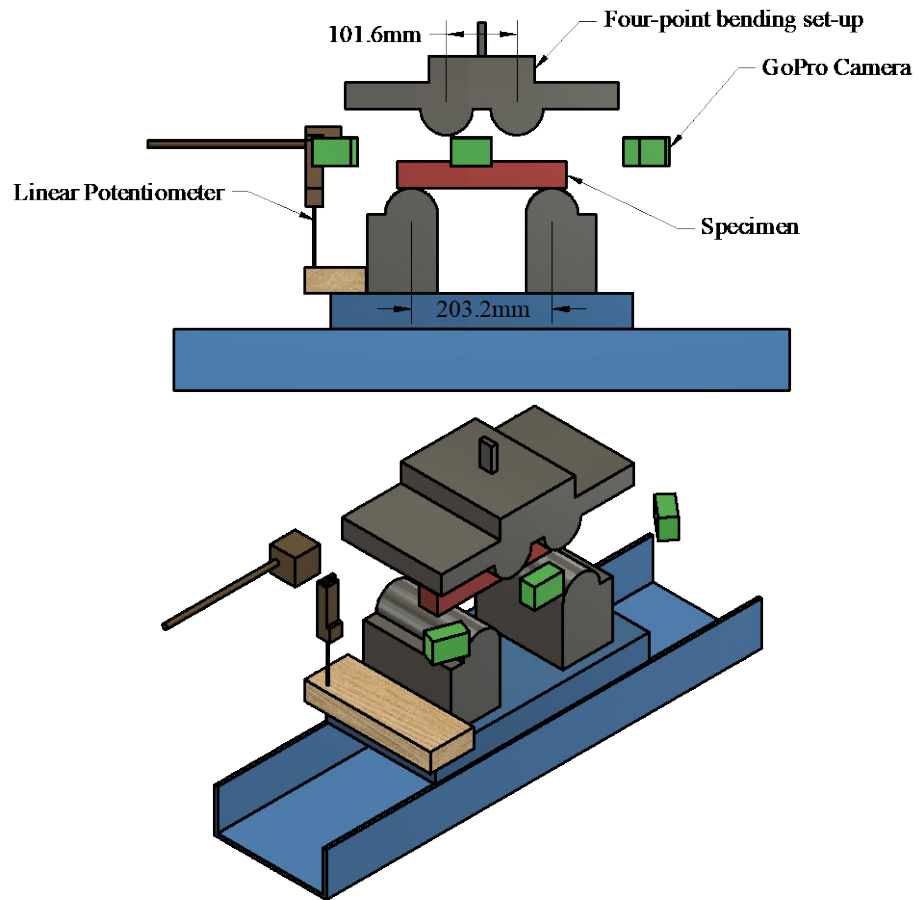
Figure 24: Diagram of the four-point bending test set-up

Figure 25: Complete test set-up: shown in the image are Go-pro cameras, linear potentiometer, and the Forney's machine

The wooden block shown in Figure 24 and 25 is clamped to the bottom plate. The wooden block touches the linear potentiometer (L-POT) that is attached to the Forney machine by a magnet and connected to the data acquisition system to record the displacement of the bottom plate as force is applied. The data acquisition system was programmed to record the displacement data every second.
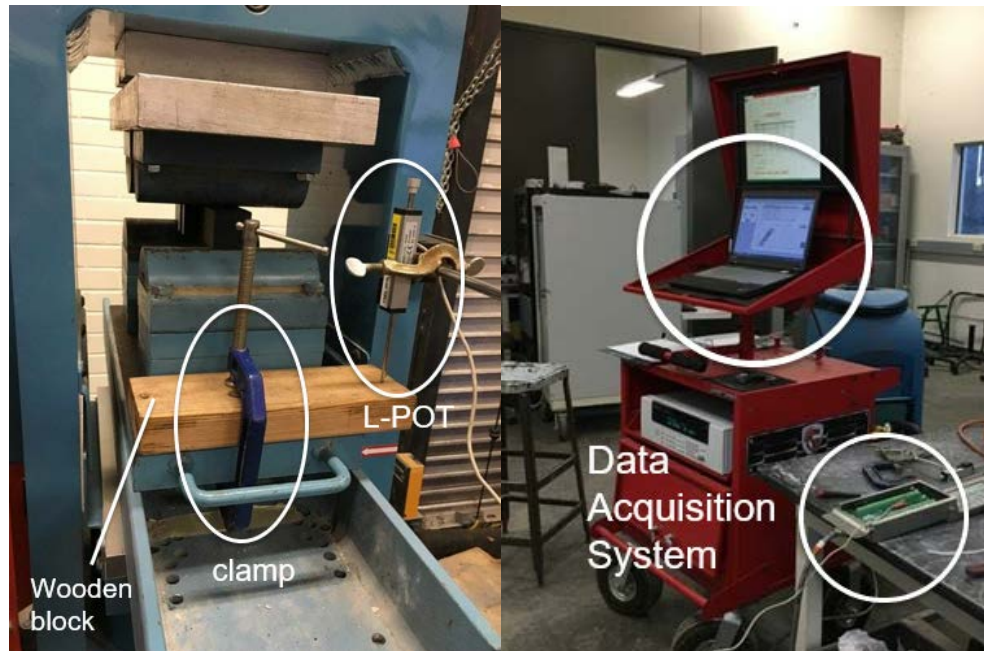
Figure 26: Linear potentionmeter (left) and data acquisition system (right)

A ramp rate of 2.5 psi per second was applied to collect enough force and displacement data before failure. Also, a pre-load of 100 lb was applied to make sure the specimen and the top and bottom plate were touching and tightly engaged before additional load was applied.

4.2. Go-Pro Camera

Go-pro cameras were mounted on each side of Forney machine to take pictures of the specimen during the test. A total of four cameras with custom 3D printed arms were clamped to the side of the Forney's machine to take pictures of the deflecting sample every second from the beginning to the end of the test. These photos were taken to observe the physical change of the specimen in detail at any time of the test to identify when and where the crack or deformation first occurred. One camera was positioned to have a frontal view of the specimen, two cameras were positioned to the sides of the specimen for an angled view, and one camera was positioned to have an angled view of the back side of the specimen. The wifi function of cameras were turned on and the images were monitored during testing through the Go-pro camera app on a mobile phone. The cameras were turned on and off by a remote controller. Since the Go-pro cameras had a battery life of approximately 2.5 hours and the SD card had a limited storage capacity, the batteries and the SD cards were replaced after every test as taking pictures every second for more than 10 minutes used a lot of memory space.
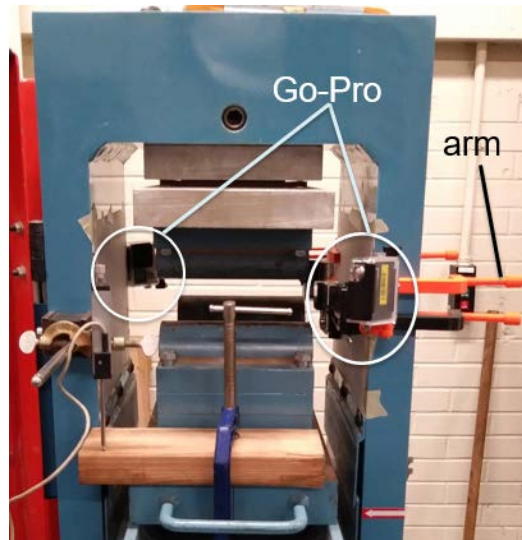
Figure 27: Go-Pro Camera set-up

4.3. Loading of Specimen

To start the test, a specimen was aligned on the bottom plate. It was centered and checked to see if the distance from the point of contact to end of the specimen was of equal length for both end. Then the "Jog Advance" button was pressed in the Forney machine software to raise the bottom plate until the top plate barely touched the specimen. The monitor for the linear potentiometer was turned on to make sure the displacement was constant. The "Tare Load" button was pressed to zero the load. To begin the test, one person pressed the Start Test button of the Forney machine and the other person pressed the Start Recording tab of the data acquisition system and the start button of the remote for all four Go-pro cameras all at the same time.
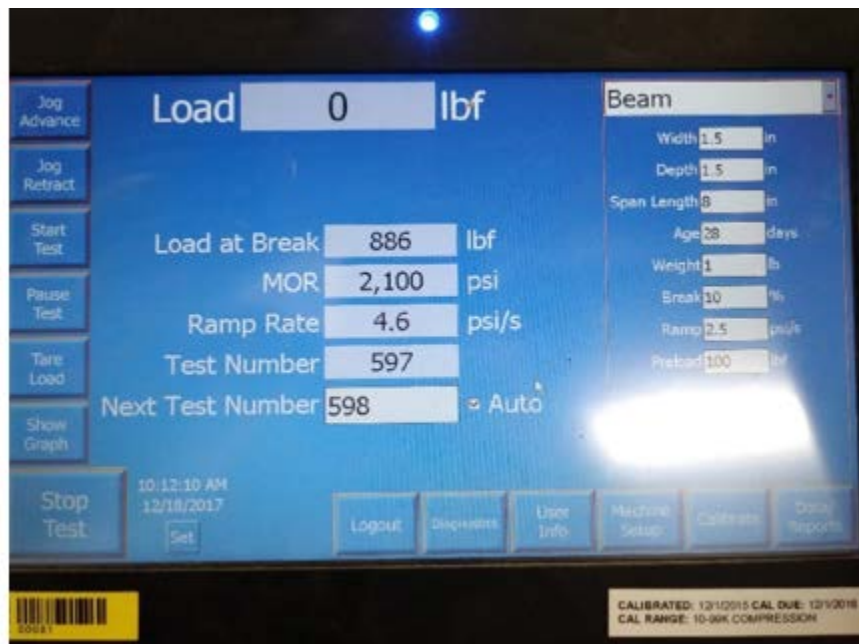
Figure 28: Screen showing the data input and output of the Forney Compression Machine

The test was stopped automatically when the Forney machine detected failure (i.e., a drop in load carrying capacity) in the specimen, or the "Stop Test" was button was manually pressed. After the test was over, data files were transferred from both Forney machine and the data acquisition system and backed-up on an external USB device.

The above procedure was repeated for testing all 12 specimens for each model and a solid beam. Each test was repeated carefully to match the testing condition of the previous specimen to ensure the reliability of the bending test. The result and the analysis of the collected data will be discussed in the next chapter.

5. Results and Analysis

Four different beams were tested: 1 control with no connections and the remaining beams each had a different type of "quick connection". Three specimens were tested for each type of beam. One representative load versus displacement plots will be shown for beam for purposes of characterizing their behavior. The photos of the specimen during different points of the loading are shown in the plots to document the progression of damage that was observed during the tests.

5.1. Behavior of the control beam

The control beams exhibited an almost linear relationship between the load and the displacement as shown in Figure 29. The maximum load was around 2000 lb and once this maximum load was reached failure immediately followed. The beam failure was very brittle and the failure occurred at one side of the contact with the top plate as shown in Figure 30.
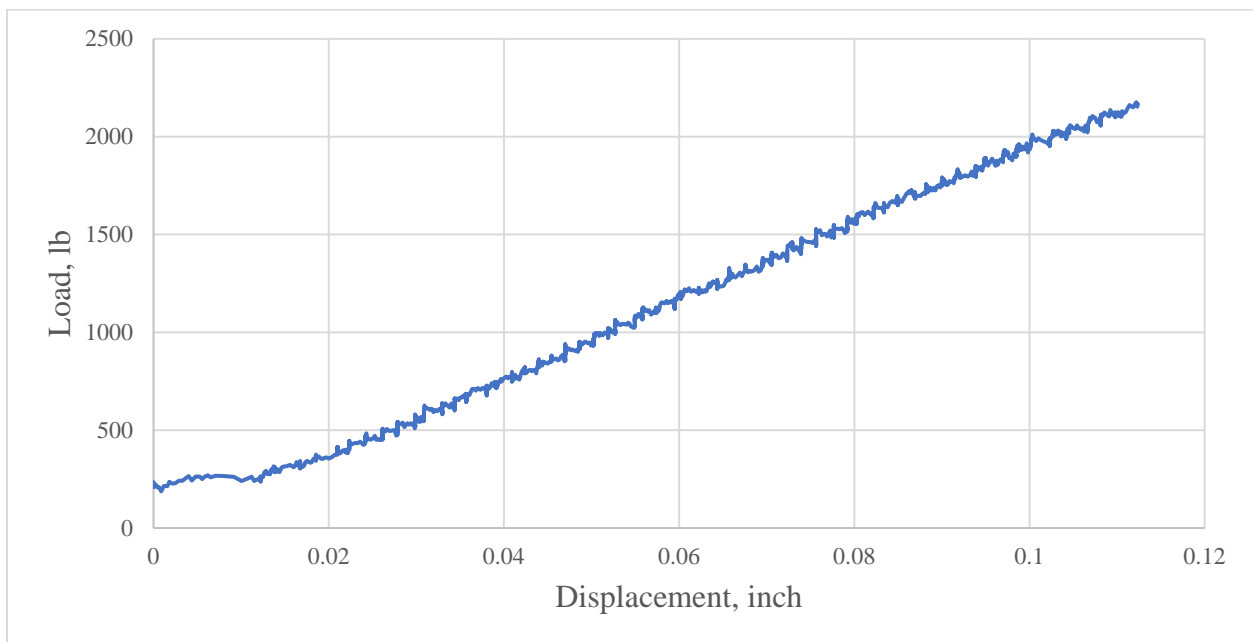
Figure 29: Load vs Displacement graph of 70% infill beams 1

Figure 30: 70% infill beam before (top) and after (bottom) failure

5.2. Behavior of the Kawaii connection

The Kawaii connection displayed a brittle behavior during the test. As shown in Figure 31, the failure occurred at the protruded tip of the connection which turned out to be the weakest plane. It is observed that the crack forms horizontally in the direction of the layer and changes its direction perpendicular to the layer before the connection fails, as shown in Figure 32 and 33.
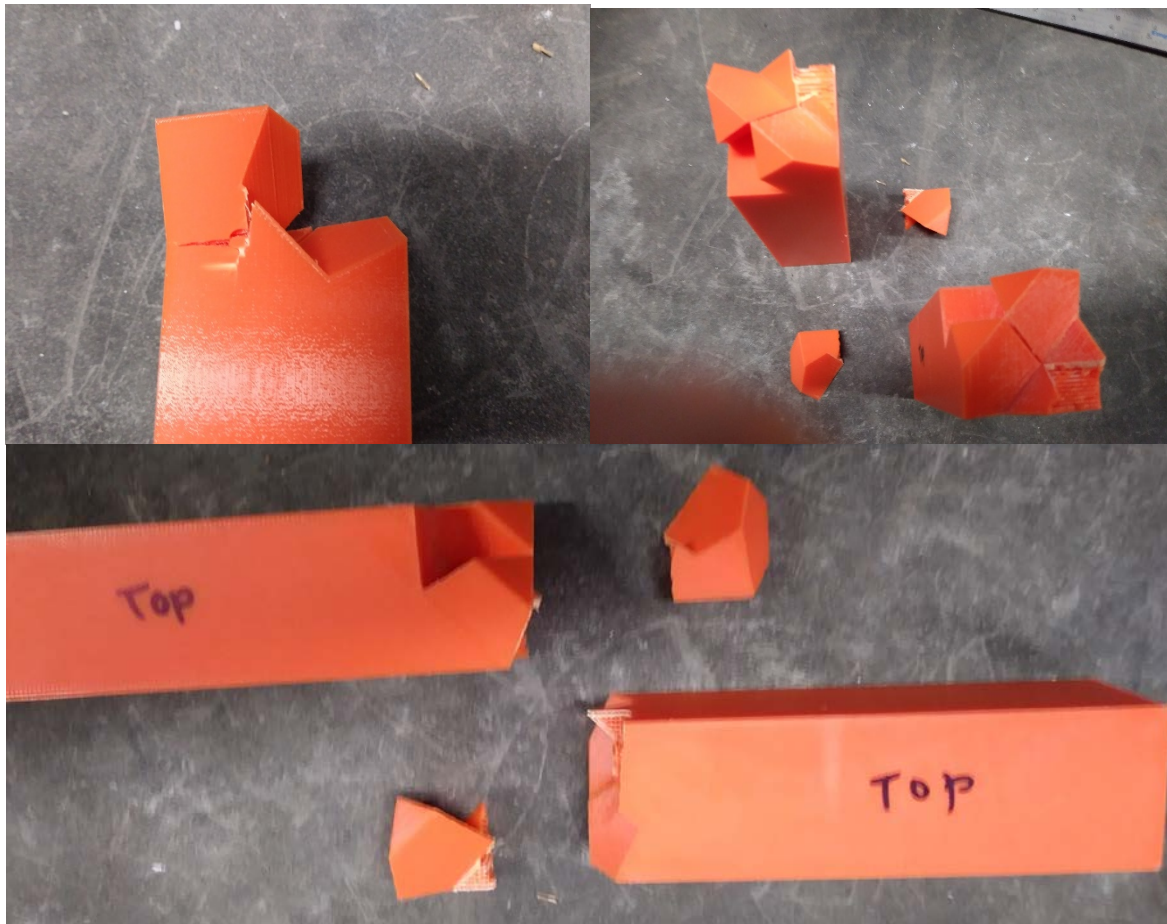
Figure 31: Kawaii connection after failure
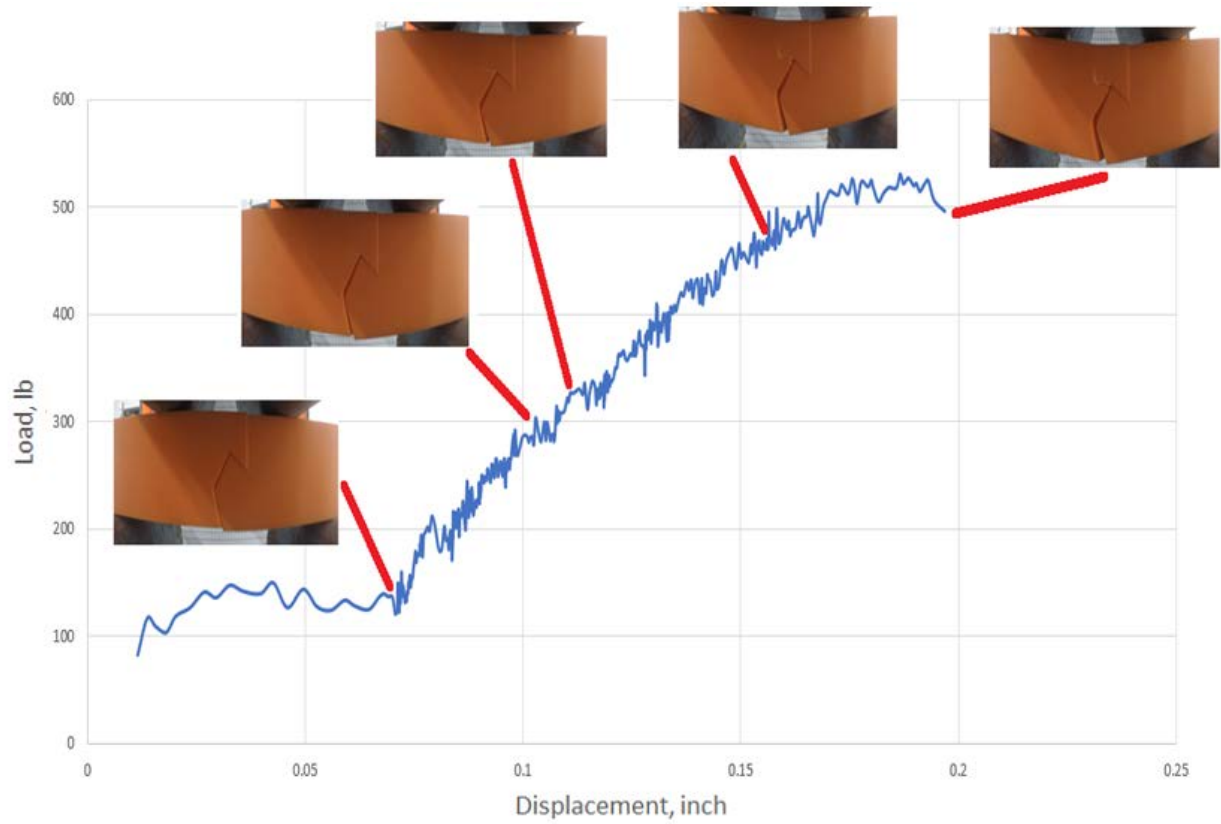
Figure 32: Crack Propagation at each load and displacement of the Kawaii connection
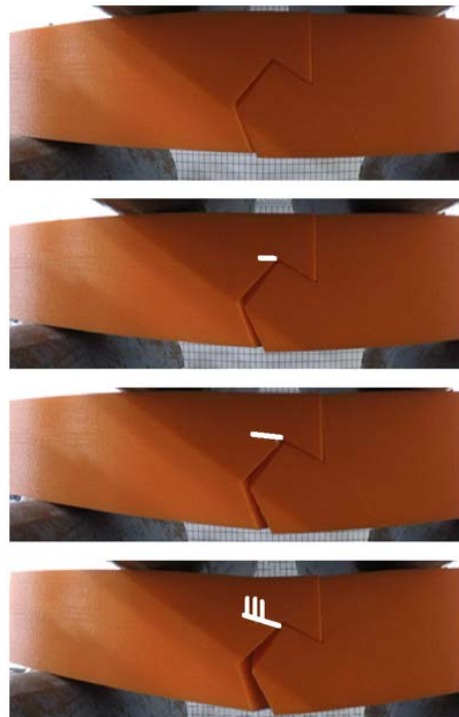
Figure 33: Crack propagation indicated by the white line

5.3. Behavior of the Shippasami connection

The Shippasami connection displayed a brittle behavior during the test as the load dropped suddenly at failure, as shown in Figure 35. The failure occurred at the tooth of the connection which turned out to be the weakest plane, as shown in Figure 34. It is observed that the crack forms perpendicular to the direction of the layer and continues to the surface of the beam as shown in Figure 36. The gaps in the connection widens rapidly after the connection reaches the maximum deflection.

Figure 34: Failure of the Shippasami connection

Figure 35: Crack propagation at each load and displacement of the Shippasami connection
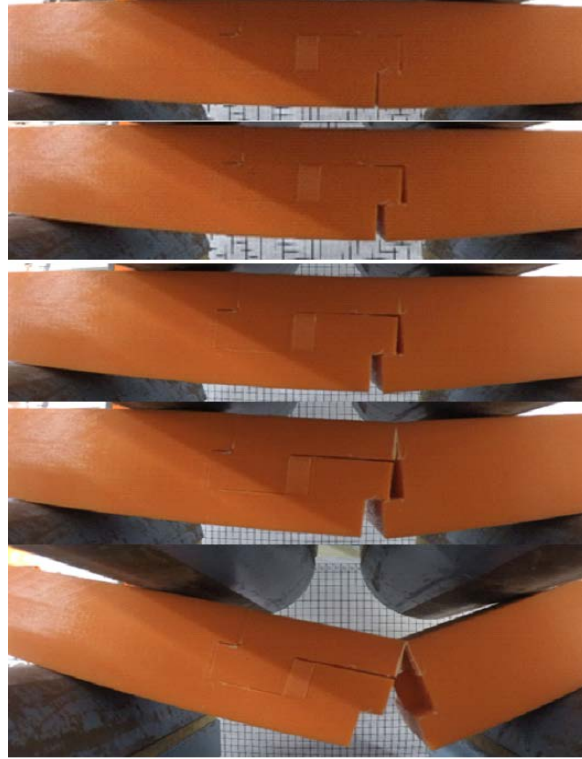
Figure 36: Crack propagation of the Shippasami connection

5.4. Behavior of the ConXTech connection

The ConXTech connection displayed a brittle behavior during the test. As shown in Figure 37, the failure occurred at the tenon head of the connection which turned out to be the weakest plane and was separated from the tenon neck. It is observed that the crack forms horizontally in the direction of the layer and continues to grow until the connection is subject to the maximum load as shown in Figure 38 and 39. The crack grows rapidly after the maximum load and stops once maximum deflection is reached.
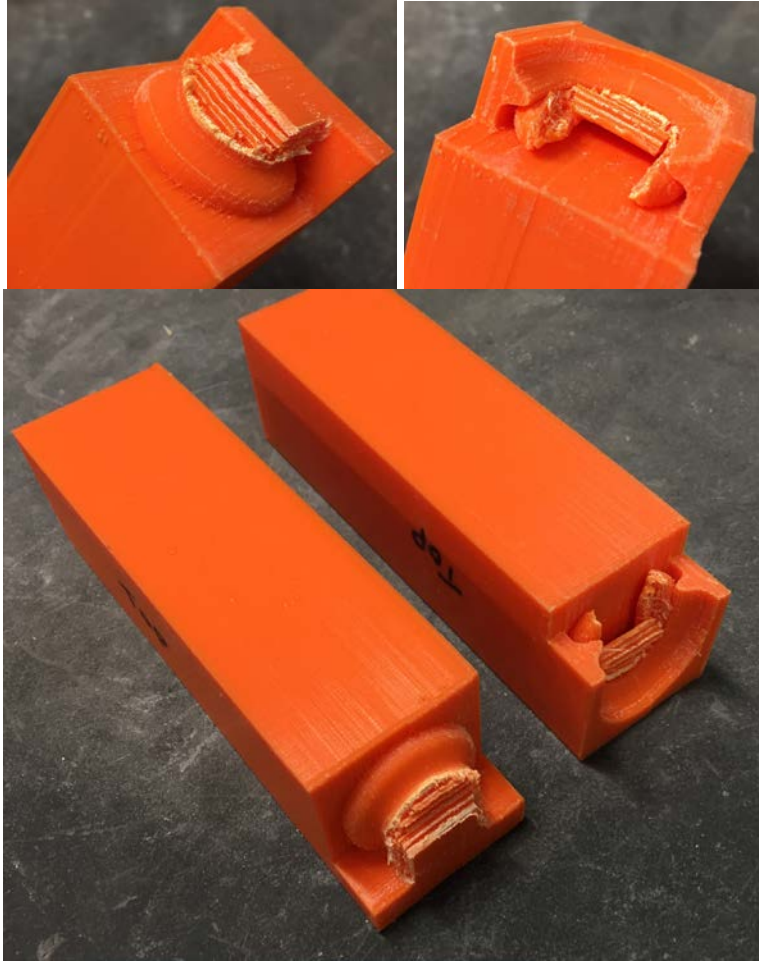
Figure 37: Failure of the ConXTech connection

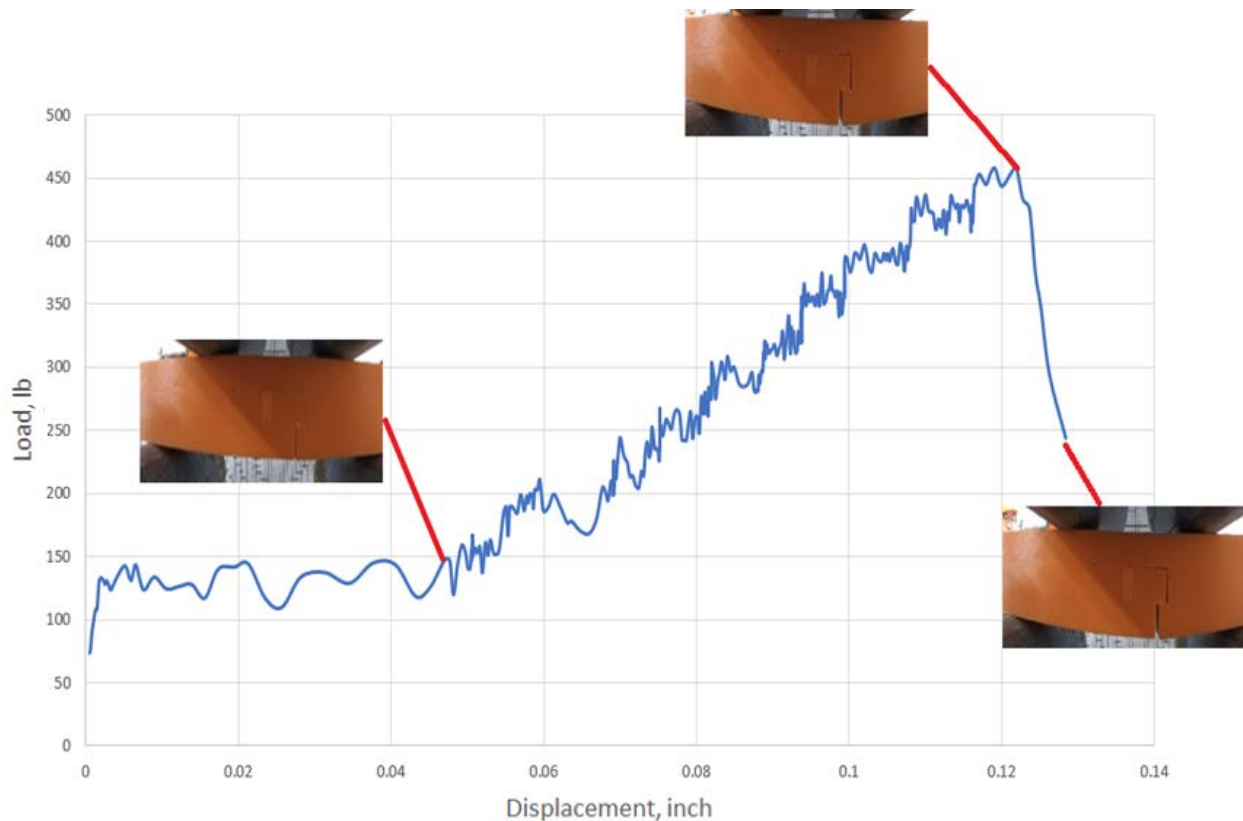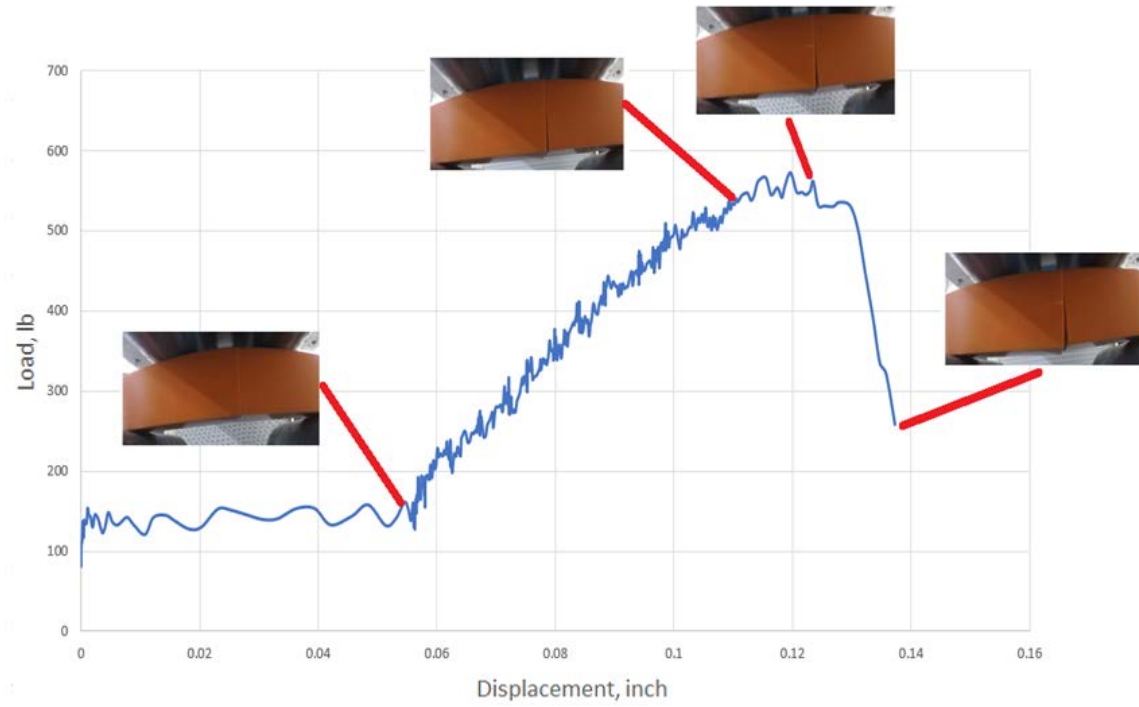*Figure 38: Crack propagation at each load and displacement of the ConXTech connection*
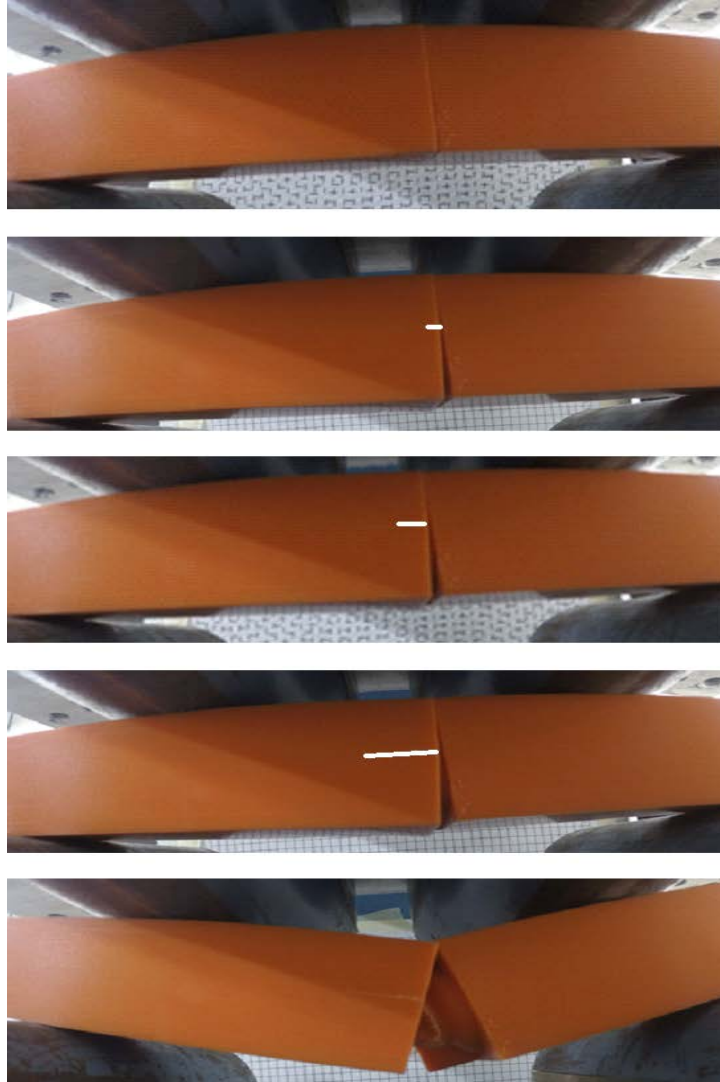
Figure 39: Crack propagation of the ConXTech connection

5.5. Analysis

Compared to the control beam, all three of the connections have a significantly lower flexural strength and higher deflection as shown in Figure 40. All three connections exhibited a flexural strength that was 20-27% of the strength of the 70% infill beam. The Kawaii and the ConXTech connection both have maximum flexural strength over 500 lb-in and a maximum deflection close to 0.2 inches. The Kawaii connection has a linear load and displacement relationship compared to the other two connections that have a part of the curve that slopes downward after they reach the point of maximum load. It is worth mentioning that typical bolted steel beam splice connections were tested in Mohr & Murray (2008) and the splice connections were on the order of 25% of the flexural strength of the solid beam with no connections [11]. Also, for non-seismic connections, AISC manual states that the end-plate connection can be designed for the required moment, but it is recommended that the connection be designed for not less than 60% of the available flexural strength of the beam [12]. Since the proposed quick connections are still able to transfer significant load, they could be suitable for non-structural applications.
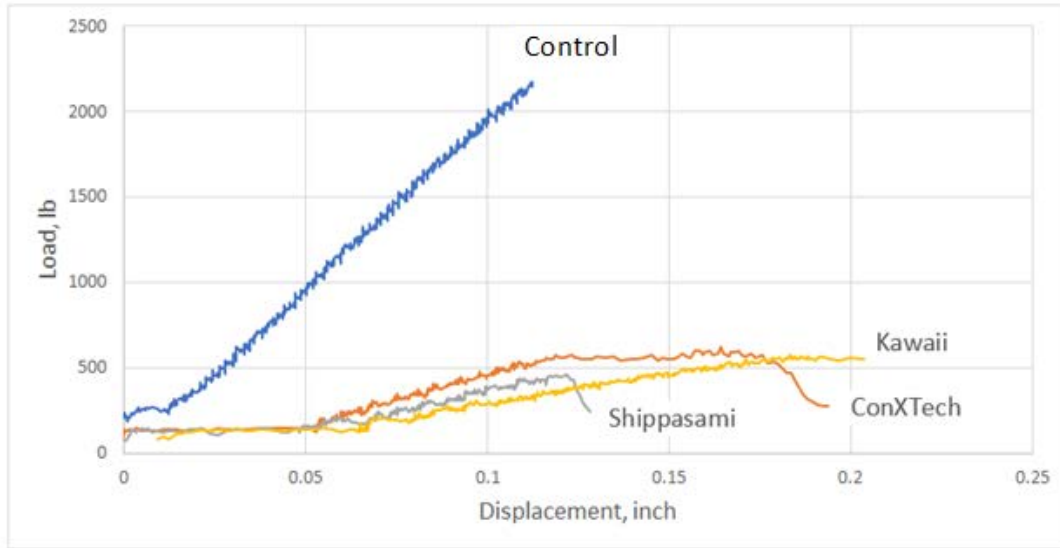
Figure 40: Load vs Displacement graph of each model

It is difficult to know what is happening in the interior of the connection during the loading, yet the location of the exterior cracks and their growth rate was consistent in all three specimens for each model. Therefore, the exterior crack propagation can be used to predict when the connection will fail. By observing the rate of growth of the crack length or the change in direction of the crack, it is possible to estimate how close the connection is to reaching its maximum load or deflection. This prediction will be very useful - especially for the Kawaii and the ConXTech connection that showed a rapid brittle failure which is not desired for a construction application. Since all of the specimen experienced total failure (when both connection parts were completely separated from each other or a piece of the connection fell off completely from its body) after the connection reached its maximum load, it is better to observe the crack patterns than to rely on the loads and deflections to estimate when the connection is going to fail.

6. Conclusion

The purpose of this study was to explore the possibility of recreating the existing connection members using the current 3D printing technology. The study created three connection models based on the traditional and modern Japanese wooden joinery and also the ConXTech connections due to their fastener-free and quick to connect configuration. From modelling the geometry of the connections in a 3D computer software to printing the actual specimens from a desktop 3D printer, the study examined the benefits and the limits of the 3D printing technology. Various failures during the printing was classified according to the type and a method to avoid each failure was noted. The study conducted a four-point bending test on the three connection models and compared the results with that of the regular solid beam of 70% print infill to assess the performance of the connection models subject to a bending load. The results showed that all three of the connection types displayed a significantly lower flexural strength than the regular solid beam and was concluded to be inadequate for structural application. Instead, due to their easiness in assembly, the ability to be custom-made and mass-produced, and their recyclable and eco-friendly nature, the 3D printed connection models in this study show more potential as a temporary, non-structural application for formwork. Another interesting observation was made while analyzing the pictures taken by the Go-Pro cameras during the test. It was found that the crack formation in the specimen of each connection model during the test had a recognizable pattern and was helpful in predicting the deflection progress and the ultimate failure of the connection.

A further study exploring the impact of different geometry and configuration of connection members on fracture toughness parameters will enhance the understanding of the properties and behavior of the joints under deformation. Also, experimenting with different types of print materials such as ABS, nylon, carbon fiber reinforced polymers, concrete and metals and different printing methods such as Stereolithography in small and large scale is necessary to fully understand the extent of the 3D printing application in the construction industry.

Appendix A: 3D printing procedures

A.1. 3D Modeling

There are several computer programs that allow 3D modeling of objects such as SketchUp (https://www.sketchup.com) and 3D Crafter (http://amabilis.com). In this project, Autodesk Fusion 360 (https://www.autodesk.com/products/fusion-360) was used as it was easier to learn for most civil engineers and architects who have used AutoCAD before. It is also freely available for students and academic institutions. All three models developed and tested in this project are modelled in Fusion 360 through rapid prototyping. The finished product is then saved as an *.STL file.

A.2. Using a 3D printer

The Cockrell School of Engineering at the University of Texas at Austin opened the Maker Studio that has 3D printers for academic and research use. The desktop 3D printer used for this study is the CraftBot XL that can print objects up to 30 x 20 x 44 cm in either PLA or ABS setting, as shown in Figure 41.

Figure 41: CraftBot XL 3D printer at the Maker Studio

Before a 3D model can be printed, it must be converted from an *.STL file to a *.gcode file that can be read by the 3D printer. CraftBot XL uses a slicer program called CraftWare that allows the user to choose print settings by selecting PLA/ABS stock materials and adjusting factors such as solid infill percentage and pattern, layer thickness, print speed, and quality. It estimates total print time and shows the print path for the user. It gives the user an option to include supports in hanging parts that may fail during the print. An example for how the CraftWare software adds supports to a model is shown in Figure 42.
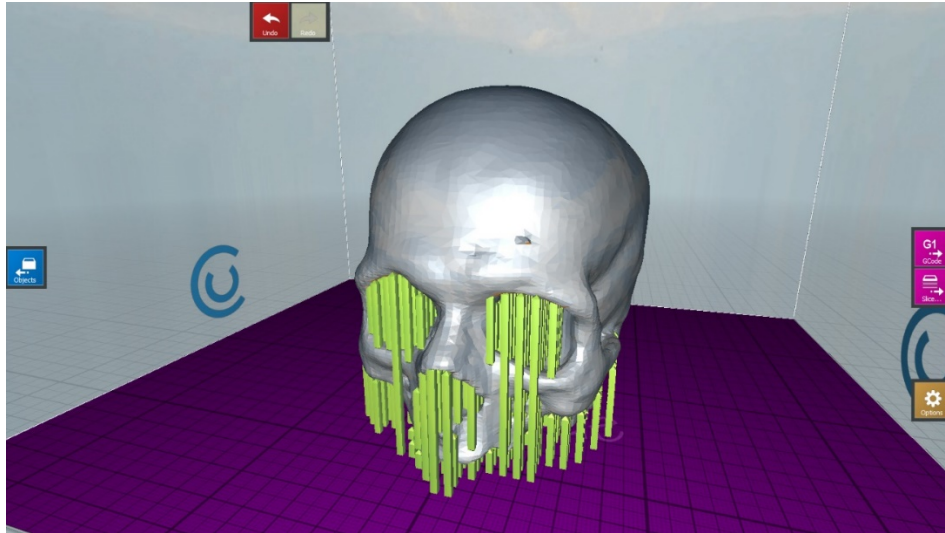
Figure 42: An example of the software is shown for a complex skull model to demonstrate specific features of Craftware [13]

It is possible to scale or rotate the object to change its orientation on the platform. CraftWare saves the file into a *.gcode format that can be saved on a USB drive and then transferred to a printer for printing.

- Solid infill percentage determines how densely the object is printed. Minimum infill is 20 percent and it can be increased all the way up to 100 percent. Higher infill means longer print time as the printer must go on an extra path to print.
- Infill pattern is how the inside of the object is printed in shape. It can be a square grid, triangle grid, 45° degree, 36° degree, or 30° degree lines, as shown in Figure 43. It is not visible from the final product as the surface of the object is completely covered in a smooth layer.
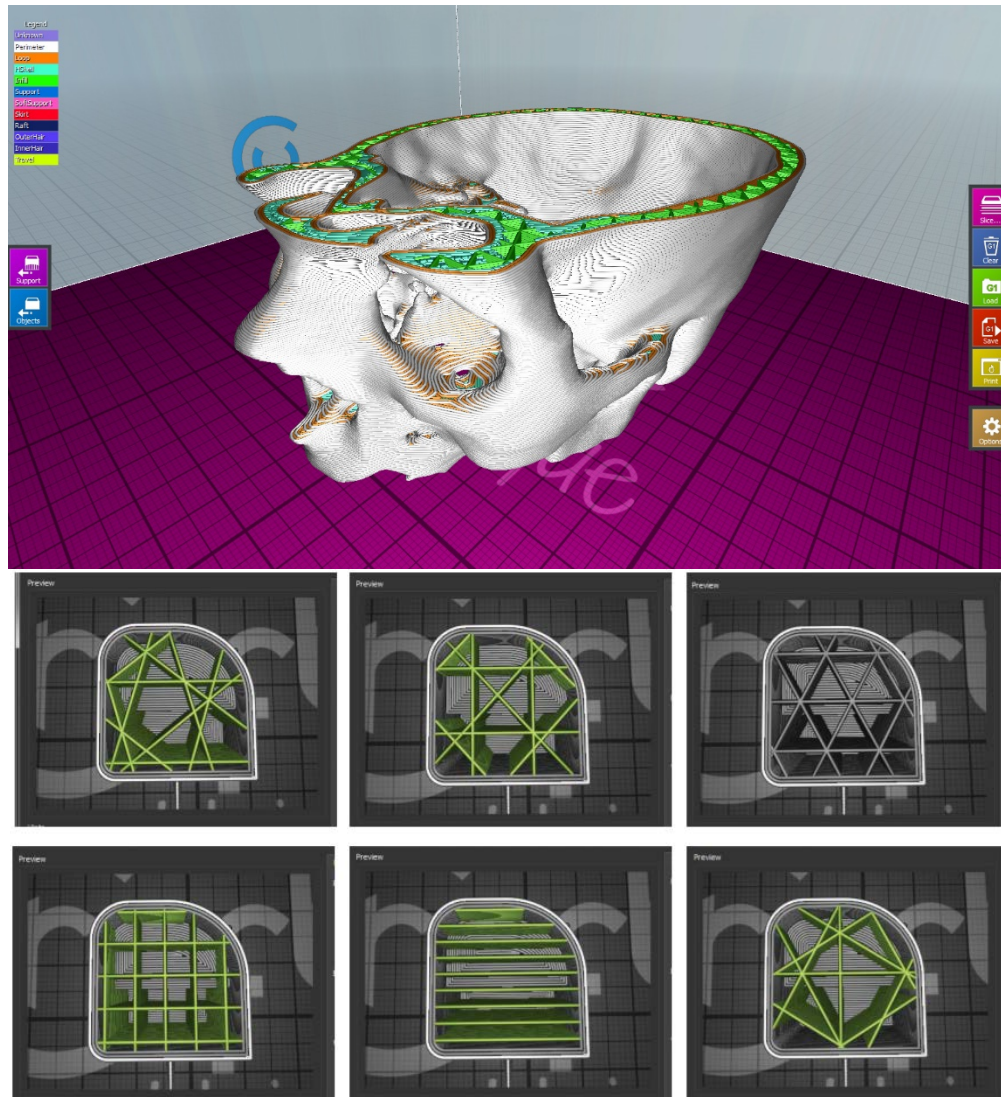
Figure 43: Traingular (top) and different infill patterns (bottom) in Craftware [13]

- Layer thickness determines the size of the filament extruded from the nozzle. Decreasing the layer thickness can improve quality as it gives more intricate detail of the object but requires longer printing time.
- Print speed determines how fast the printer head is moving to build layers. Higher print speed reduces the time and quality of the print.

Most PLA and ABS printer filaments can be easily purchased from online retailers (e.g., Amazon.com) or directly from the printer company if the printer requires a customized filament. For this project, spools of 1.75mm diameter, orange color Hatchbox PLA 3D printer filaments were used, as shown in Figure 44. The spools are individually loaded in the printer so that the filament can be extruded through the printer nozzle.

Figure 44: Hatchbox PLA printer filament [14]

Before printing begins, the platform bed is coated with a hair spray so that the first layer of the print adheres to the surface and remains level. Craftbot XL has a color touchscreen that allows the user to select the *.gcode file from the USB to be printed. When the "start print" button is pressed, the platform bed and the printer head are heated to 60 °F and 215 °F, respectively. Then the printer head moves and starts printing the first layer and continues to build layer upon layer until the print is finished. It is possible to pause the print to replace the filament spool or stop the print completely if the print fails or if the user is no longer able to monitor the print. Some of the specimens manufactured in this project required print times around 24 hours. While overnight prints are typically not allowed per Maker Studio rules, the research team received special permission from the Maker Space director and the lab manager for overnight prints for this project.

Once the print is finished, the final product can be removed from the platform using a flat scraper tool. Supports, if present, need to be removed and sanded smooth using a nail or a screw drive. The platform bed needs to be washed in water to remove any traces of filament and dried with a cloth for the next print job. The printer head also needs to be cleaned by removing any filament hanging on the side of the head or the fans.

References

[1] Butt Joint. (n.d.). Retrieved from http://www.woodworkbasics.com/butt-joint.html

[2] Mortise and Tenon. (n.d.). Retrieved from http://www.woodworkbasics.com/mortise-and-tenon.html

[3] Rebstock, F. (2015). A New concept to Join Members in Frame Construction with CNC-Fabricated Timber Beams and LVL Nodes: Strength Test and Failure Analysis. Master's Thesis, 18-25..

[4] Horyuji Temple [Western Precinct: Main hall (left), central gate (center) and five-story pagoda (right)]. (n.d.). Retrieved from https://www.japan-guide.com/e/e4104.html

[5] Sumiyoshi, Torashichi, and Gengo Matsui. Wood Joints in Classical Japanese Architecture. Kajima Institute Publishing Co., 1990.

[6] Kobayashi, S. (2014, September 19). Kawai tsugite [Digital image]. Retrieved from https://www.instagram.com/shino_bunny/?hl=en

[7] Bolted Column Splice [Moment Connection]. (n.d.). Retrieved from https://www.engr.mun.ca/~adluri/courses/steel/ppt files1/Topic -Connections -typical joints.pdf

[8] MAG welding [William Haley Engineering Ltd]. (n.d.). Retrieved from https://www.steelconstruction.info/Welding

[9] ConXR200 [Digital image]. (n.d.). Retrieved from http://www.conxtech.com/

[10] Rebstock, F. (2015). A New concept to Join Members in Frame Construction with CNC-Fabricated Timber Beams and LVL Nodes: Strength Test and Failure Analysis. Master's Thesis, 18-25.

[11] Mohr, Benjamin A.; Murray, Thomas M. (2008). "Bending Strength of Steel Bracket and Splice Plates," Engineering Journal, American Institute of Steel Construction, Vol. 45, pp. 97-106.

[12] American Institute of Steel Construction. (2011). Steel Construction Manual, 14th Ed. (Table 1-22). Chicago: AISC.

[13] Craftware [Digital image]. (n.d.). Retrieved from https://craftunique.com/craftware/

[14] 1kg spool [Digital image]. (n.d.). Retrieved from https://hatchbox3d.com